Chemical Engineering Journal 150 (2009) 122–130

Contents lists available at ScienceDirect

Chemical Engineering Journal

journal homepage: www.elsevier.com/locate/cej

Biosorption of acidic dyes from aqueous solution by *Paenibacillus macerans*: Kinetic, thermodynamic and equilibrium studies

Ferdağ Çolak[a], Necip Atar[b], Asim Olgun[b,*]

[a] *Department of Biology, Faculty of Arts@science, University of Dumlupinar, Kütahya, Turkey*
[b] *Department of Chemistry, Faculty of Arts@science, University of Dumlupinar, Kütahya, Turkey*

ARTICLE INFO

Article history:
Received 24 October 2007
Received in revised form 11 July 2008
Accepted 4 December 2008

Keywords:
Biosorption
Paenibacillus macerans
Acidic dye
Isotherms
Langmuir

ABSTRACT

Batch studies were conducted for thermodynamic, kinetics and equilibrium studies on the biosorption of Acid Blue 225 (AB 225) and Acid Blue 062 (AB 062) from aqueous solution by *Paenibacillus macerans*. The operating variables studied were initial dye concentration, biomass concentration, contact time, temperature and solution pH. Results show that the pH value of 1 is favorable for the biosorption of dyes. The biosorption data have been analysed using Langmuir, Freundlich and Tempkin isotherms. The isothermal data for biosorption followed Langmuir Model. The biosorption processes conformed to the pseudo-second-order rate kinetics. Thermodynamic parameters such as *enthalpy*, *entropy*, and *Gibb's free energy changes* were also calculated and it was found that the biosorption of dyes by *Paenibacillus macerans* was a spontaneous process. The biosorption mechanism of biomass was explained by FT-IR spectroscopy and the FT-IR spectrum confirmed the presence of –COOH, C=O, and $-NH_2$ groups in the biomass structure. The maximum adsorption efficiency of AB 225 and AB 062 is 94.98 mg g^{-1} and 95.08 mg g^{-1}, respectively.

1. Introduction

Dye wastewater discharged from textile and dyestuff industries are important sources of contamination responsible for the continuous pollution of the environment. Wastewaters containing dye may be toxic and even carcinogenic and this posses a serious hazard to aquatic living organisms [1–5]. The removal of colour from dye bearing effluents is one of the major problem due to the difficulty in treating such wastewaters by conventional treatment methods [6,7]. Various physical, chemical, and biological methods, namely adsorption, biosorption, coagulation, precipitation, membrane filtration, solvent extraction, chemical oxidation have been used for the treatment of dye-containing wastewater [8–10].

Of the dyes, the water-soluble reactive and acid dyes are the most problematic because of their tendency of passing through conventional treatment systems unaffected. Hence, their removal is also of great importance [11–15]. Since the 1980s, biosorption has been continuously investigated for the removal of heavy metals and other organic pollutants including dyes [16]. The process of uptake of solute using biomaterials (microbial cells), whether dead or alive, is known as biosorption [17]. Aksu and Tezer [14] studied with dried *R. arrhizus* for the removal of Remazol Black B, a reactive anionic dye from aqueous solution. Fu and Virarahavan [18–22] studied the removal of Basic Blue 9 (cationic), Acid Blue 29 (anionic), Congo Red (anionic), and Disperse Red 1 (nonionic) dyes from aqueous solutions by biosorption on dead and pretreated *Aspergillus niger* fungus. They found that *A. niger* is capable of removing dyes from an aqueous solution. They suggested that three major functional groups: carboxyl, amino and phosphate, and the lipid fraction in the biomass of *A. niger* played an important role in the biosorption of these dyes [18–22]. These results showed that the use of biomaterials as sorbents for the treatment of wastewaters would provide as a potential alternate to the conventional treatment methods [23].

The present work investigates the potential use of *Paenibacillus maceran biomass as adsorbent* for the biosorption of AB 225 and AB 062 from aqueous solutions. The effects of biosorbent dosage, contact time, pH, and initial dye concentration on the biosorption of AB 225 and AY 220 onto *Paenibacillus macerans* were investigated. Furthermore, the isotherms, kinetics and thermodynamics data were evaluated.

2. Materials and methods

2.1. Isolation of endospore forming bacilli

Preparation of the guts was carried out under sterile conditions. Prior to dissection, the animals were submerged in 70% aqueous ethanol for 2 s in order to avoid contamination of the isolation plates with microorganisms attached to the outer surface of the animals. Following dissection, each sample was placed in a microtube filled with 250 μl sterile saline (0.9%, w/v) and carefully crushed mechanically from which a suspension was prepared using a vibra-

* Corresponding author. Tel.: +90 274 2652051; fax: +90 274 2652056.
E-mail address: aolgun@dumlupinar.edu.tr (A. Olgun).

1385-8947/$ – see front matter © 2009 Published by Elsevier B.V.
doi:10.1016/j.cej.2008.12.010

tion shaker. Brain heart infusion (BHI) agar (Merck), a nutrient-rich complex medium for cultivation of fastidious microorganisms, and nutrient agar (NA) (Merck) were used as isolation medium. About 100 μl of each suspension was plated on BHI agar and NA plate. Plates were incubated aerobically at 37 °C. After an incubation periods of 3 days, the colonies were selected for isolation.

2.2. Identification of isolate

For identification at genus level of isolates their morphological and some biochemical properties were determined by carrying out the Gram stain, endospore stain and catalase test, in accordance with Bergey's Manual of Systematic Bacteriology [24]. Identification at species level of the *Bacillus* isolates was based on the biochemical properties (VITEK system) and fatty acid methyl ester (FAME) profiles.

The Vitek *Bacillus* Biochemical Card (bioMerieux Vitek, Inc., Hazelwood, MO) was used as an essential method for identification of the species level. The procedure for the performance of the Vitek Card test was in accordance with that described by the manufacturer. To determinate anaerobic growth, the isolates were inoculated plates of Anaerobic Brewer Agar (Merck) and incubated in an anaerobic jar at 37 °C for 1–2 days [24].

FAMEs were extracted from the isolates using standard and recommended procedures for gas chromatographic (GC) FAME analysis. Analysis was performed with a Hewlett-Packart 6890 Series Gas Chromatography and the Sherlock Microbial Identification System software (MIDI Inc., Newark, DE, USA), employing the MIDI standard method. Identification at species level was performed by comparing the fatty acid profiles to the MIDI standard library [25].

2.3. Microorganism and growth condition

P. macerans strain was grown on NA. Cells were inoculated on Petri dishes by scratching and were left over night at 35 °C in the incubator. Cell cultures were collected from Petri dishes by the aid of serum physiologic and were harvested by means of centrifugation at 13,000 rpm for 5 min, then were washed twice with serum physiologic. The pellets were put in Petri dishes and dried at 70 °C for 24 h.

2.4. Preparation of dye solution

The dyes used in this study were AB 225 and AB 062 obtained from a textile company in Istanbul, Turkey and used without further purification. The chemical structures and general data of these dyes are displayed in Fig. 1 and Table 1, respectively. The dye stock solutions were prepared by dissolving accurately weighted dyes in distilled water to the concentration of 1000 mg l^{-1} and the experimental solutions concentrations were obtained by dilution.

2.5. Measurements of dye uptake

All experiments were carried out with biosorbent samples (1 g l^{-1}) at 25 °C in 50 ml beakers in an IKA magnetic stirrer operating at 200 rpm to elucidate the optimum conditions (pH, contact time and initial dye concentration). Before analysis of the dye concentration, samples were centrifuged at 4000 rpm for solid–liquid separation. Concentration of the dye in solution was analysed using a Shimadzu UV-1700 Double Beam. Earlier the wavelength at which maximum absorbance λ_{max} (nm) occurred for each dye in aqueous solution was determined by performing full range of (200–900 nm) wavelength scans. Concentrations of dyes in solution were estimated quantitatively using the linear regression equations obtained by plotting a calibration curve for each dye over a range of concentrations. The dye adsorption capacities of biosorbent were determined at a certain time intervals (10, 20, 30, 45, 60, 90, 120, 150, and 180 min) and at various temperatures (25–55 °C). The equilibrium was established after 90 min. The effect of pH on biosorption was studied by adjusting dye solutions (100 mg l^{-1}) to different pH values (1–10) and agitated with 1 g l^{-1} of biosorbent for 90 min. The dye solutions were adjusted to the required initial pH values with the addition of HCl or NaOH (1 M). Dye adsorption experiments were also accomplished to obtain isotherms at various temperatures (25–55 °C) and to a range of 50–300 mg l^{-1} dye concentrations. The amount of dye adsorbed by biosorbent, q_e (mg g^{-1}), was calculated by the following mass balance relationship:

$$q_e = \frac{(C_0 - C_e)V}{W} \quad (1)$$

where C_0 and C_e are the initial and equilibrium dye concentrations in solution, respectively (mg l^{-1}), V the volume of the solution (l) and W is the mass (g) of the adsorbent used.

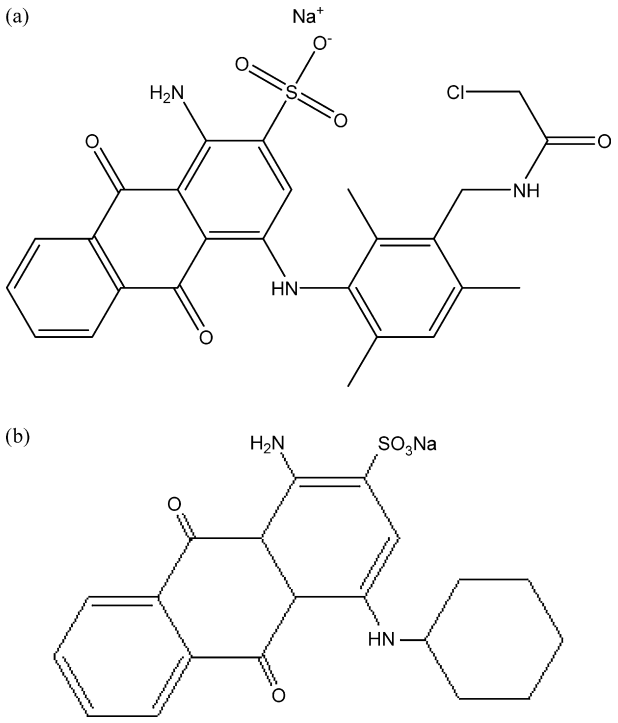

Fig. 1. Molecular structure of Acid Blue 225 (a) and Acid Blue 062 (b).

Table 1
Properties of Acid Blue 225 and Acid Blue 062.

Dye properties	Acid Blue 225	Acid Blue 062
λ_{max} (nm)		635
Type	Anionic	Anionic
M_w (g mol^{-1})	563.99	401.46

2.6. Zeta potential measurements

The zeta potential of *P. macerans* was determined by an electroacoustic technique with a Zeta Probe Analyzertm (Zeta Meter 3.0) at room temperature. Known amount of the biosorbent was suspended in 50 ml of deionized water and solution pH was adjusted to between 1.0 and 10.0 using either 0.1 M HNO_3 or 0.1 M NaOH. After pH adjustment, the mixtures were equilibrated in a magnetic stirrer for 20 min and then the zeta potential was measured.

2.7. Infrared spectroscopic analysis

Samples of 50 mg KBr disks containing 2% of finely ground powder of the each sample were prepared and then recorded Bruker Vertex 70 FT-IR spectrometer equipped with the harric MVP2-unit in the range of 4000–500 cm^{-1} region in order to investigate the functional groups present in the biomass.

3. Results and discussion

3.1. Characteristic of biosorbent

In this study, isolated gut of Coleptera (32AaB2) by FAME was identified as *P. macerans*. There upon anaerobic growth of the isolate was investigated and it was found that it exhibited anaerobic growth. The biochemical properties and fatty acid profile of *P. macerans* 32AaB2 are as shown in Tables 2 and 3, respectively.

3.2. Effect of pH

The pH of the aqueous solution is an important controlling parameter in the adsorption process of textile dyes. The initial pH of the dye solutions was investigated over a range from 1 to 10. As shown in Fig. 2, the uptake of anionic dyes increased with a decrease in the solution pH. The maximum uptake levels of AB 225 and AB 062 were observed as 89.92 mg g^{-1} and 91.71 mg g^{-1}, respectively, at pH 1.0. It is well known that at lower pH, more protons will be available to protonate the adsorbent surface, thereby increasing the electrostatic attractions between negatively charged dye anions and positively charged adsorption sites and causing an increase in the dye adsorption [26].

The zeta potential, which corresponds to the surface charge of solid, is one of the most essential factors in the biosorption reaction.

Table 2
Identification and biochemical properties (VITEK) of isolate.

Negative control	–
Sucrose	+
Tetrazolium red	+
Tagatose	–
Glucose	+
Inositol	–
Galactose	–
Arabinose	–
Xylose	+
Mannitol	+
Raffinose	–
Salicin	+
Amigdalin	+
Inulin	+
Ribose	+
Maltose	+
Trehalose	+
Palatinose	+
Sorbitol	+
N-acetyl-D-glucosamine	+
Amylopectin	–
Potassium thiocyanate	+
%7 sodium chloride	+
Mandelic acid	+
Oleandomycin	–
Sodium acetate	+
Arabitol	–
Polyamidohygro streptin	+
Nalidixic acid	–
Esculin	+
Anaerobic growth	+
Species	*P. macerans*

Table 3
Identification and fatty acid profiles (FAME) of isolate.

Fatty acids	32AaB2% range
13:0 ISO	0.48
14:0 ISO	0.68
14:0	2.22
15:0 ISO	26.38
15:0 ANTEISO	34.79
16:0 ISO	1.20
16:1w11c	3.99
16:0	12.70
ISO 17:1 w10c	1.60
17:1 ISO I/ANTEI B	–
17:0 ISO	8.51
17:0 ANTEISO	6.54
18:0	0.92
Similarity index	0.844
Species	*P. macerans*

Fig. 3 shows the surface charge of the biomass at different pH. The maximum positive zeta potential value of *P. macerans* was recorded at pH 1.0, which corresponded to maximum biosorption efficiency of the acidic dyes. The zeta potential values of the biomass was observed as negative at the pH 10 .0 and the overall surface of the biomass was positively charged at the pH values between 1.0 and 3.0. This finding shows that strong electrostatic attraction exists between the surfaces of *P. macerans* and acidic dye at low pH values. For this reason, the pH value of 1.0 in dye solutions were selected as optimum pH for the other experiments.

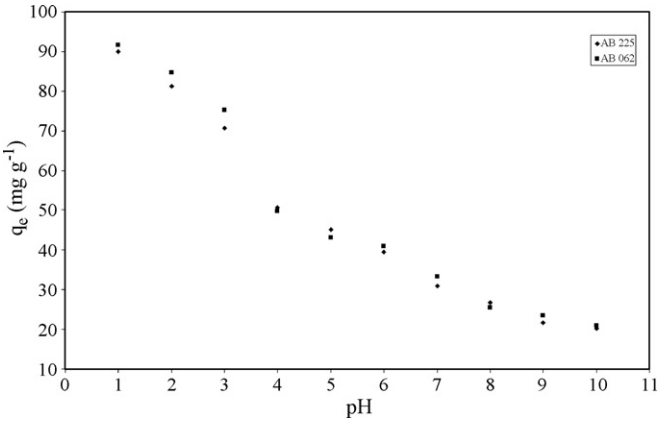

Fig. 2. Effect of pH on the removal of AB 225 and AB 062 by *P. macerans*.

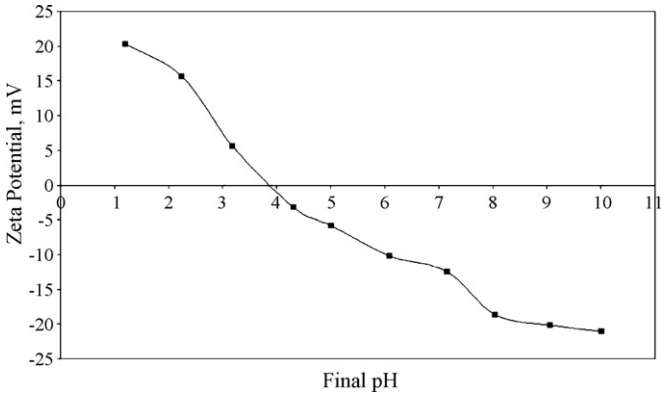

Fig. 3. Variation of zeta potential of *P. macerans* with pH.

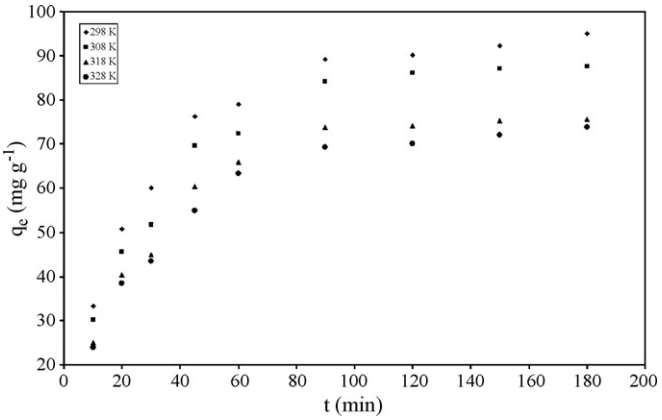

Fig. 4. Effect of contact time on the removal of AB 225 by *P. macerans* at various temperatures.

3.3. Effect of contact time and temperature

The effects of contact time at various temperatures on the biosorption of acidic dyes are depicted in Figs. 4 and 5. The experiments carried out at the pH value of 1.0 at 1 g l^{-1} biomass concentration at 50 ml of 100 mg l^{-1} initial dye concentration at the temperature range of 25–55 °C. As can be seen from the figures, when the contact time was increased, the amount of biosorption was not drastically increased. The sorption equilibrium was reached in 90 min. After this time, biosorption rate was slow leading to a single, smooth and continuous saturation curve. As shown in the figures, the decrease of the equilibrium uptakes with further increase in temperature means that the dye biosorption process is exothermic. The biosorption is favored by a decrease in temperature, a phenomenon which is also characteristic of physical adsorption. Similar results were observed by Aksu and Tezer [14], who investigated the effect of temperature on the biosorption of Remazol Black B reactive dye by *R. arrhizus* and indicated that adsorption decreases with increasing temperature. Gallagher et al. [27] also found that biosorption of Reactive Brilliant Red by *R. oryzae* was a physical adsorption due to increase of biosorption capacity with decreasing temperature.

3.4. Effect of biosorbent dosage

The effect of biosorbent dosage on the biosorption of AB 225 and AB 062 is shown in Fig. 6. The biosorption experiments carried out at seven different biosorbent concentrations at pH of 1.0, and contact time 90 min and 25 °C, using 50 ml of 100 mg l^{-1} dye solution for both AB 225 and AB 062 to investigate the effect of biosorbent concentrations. As shown in Fig. 6, the amount of dye adsorbed increased with an increase in the adsorbent concentration. The dye removal of *P. macerans* was found to be negligible after dosage of 1 g l^{-1}.

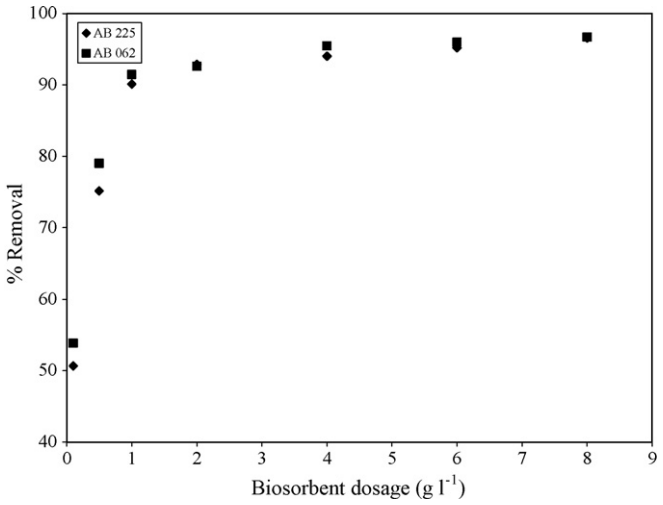

Fig. 6. Effect of biosorbent dosage on the removal of AB 225 and AB 062 by *P. macerans*.

3.5. Effect of dye initial concentration

The initial concentration provides an important driving force to overcome all mass transfer resistance of all molecule between the aqueous and solid phases [28–32]. The effect of the initial concentration of AB 225 and AB 062 in the solutions on the rate of biosorption onto *P. macerans* was studied at the pH value of 1.0 at 1 g l^{-1} biomass concentration using acidic dye solutions ranged from 50 mg l^{-1} to 300 mg l^{-1}. Figs. 7 and 8 indicate that the uptake of dye increased with increasing initial dye concentrations up to 100 mg l^{-1} for AB 225 and AB 062 dyes, respectively, and then it remained unchanged by further increase in initial dye concentrations. These results suggest that the available sites on the biosorbent are the limiting factor for dye biosorption.

3.6. Biosorption kinetics

In order to analyze the biosorption kinetics of acidic dyes, the first-order, the pseudo-second-order and intraparticle diffusion

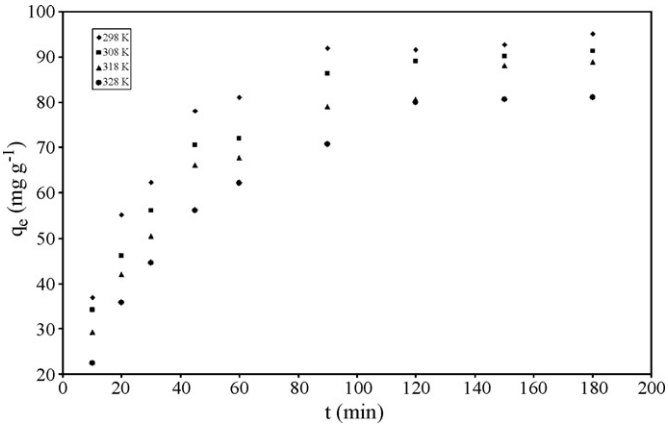

Fig. 5. Effect of contact time on the removal of AB 062 by *P. macerans* at various temperatures.

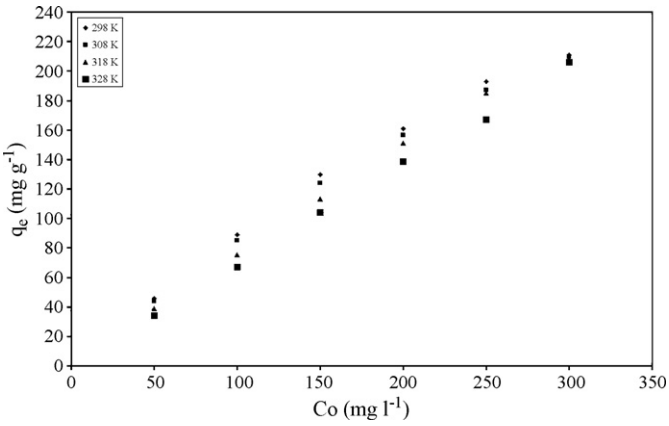

Fig. 7. Effect of dye initial concentration on the removal of AB 225 by *P. macerans*.

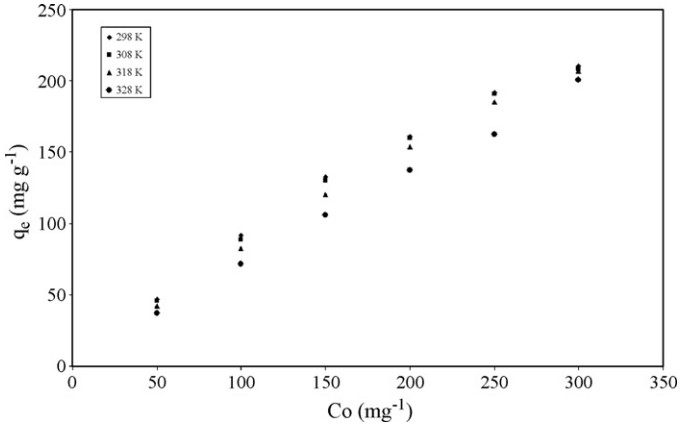

Fig. 8. Effect of dye initial concentration on the removal of AB 062 by *P. macerans*.

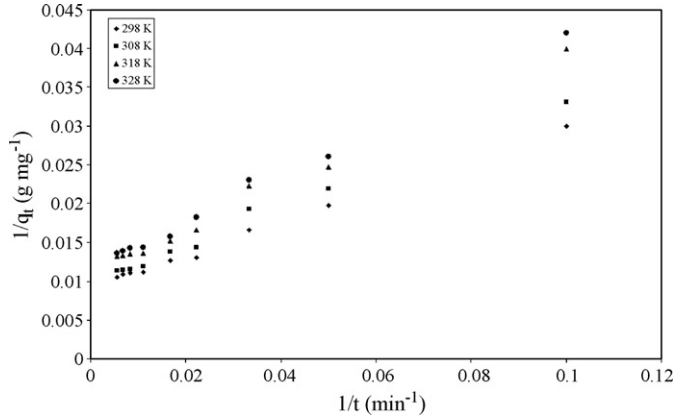

Fig. 9. First-order kinetic plots for the biosorption of AB 225 by *P. macerans* at various temperatures.

models were applied to data obtained from the experiments. The first-order rate expression [32] given as

$$\frac{1}{q_t} = \frac{k_1}{q_1}\frac{1}{t} + \frac{1}{q_1} \tag{2}$$

where q_1 and q_t are the amounts of dye ($mg\,g^{-1}$) adsorbed at equilibrium and time t, respectively, and k_1 is the rate constant of adsorption (min^{-1}) biosorption. The values of k_1 calculated from the slope of the plots of $1/q_t$ vs. $1/t$ as shown in Figs. 9 and 10.

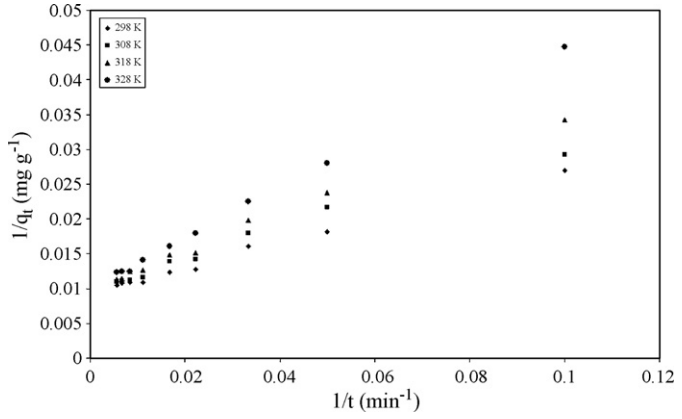

Fig. 10. First-order kinetic plots for the biosorption of AB 062 by *P. macerans* at various temperatures.

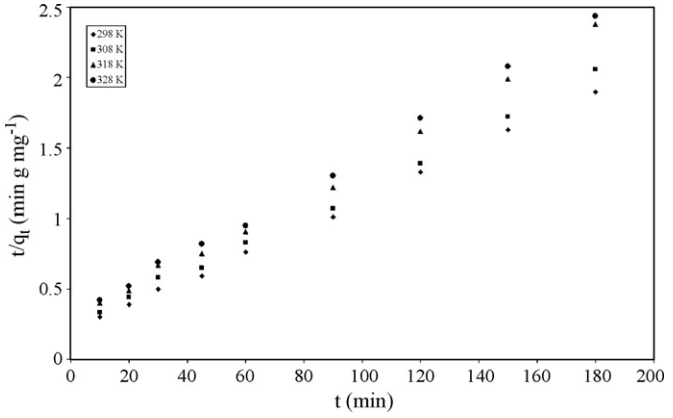

Fig. 11. Pseudo-second-order kinetic plots for the biosorption of AB 225 by *P. macerans* at various temperatures.

The pseudo-second-order kinetic model [33] is expressed as

$$\frac{t}{q_t} = \frac{1}{k_2 q_2^2} + \frac{1}{q_2}t \tag{3}$$

where q_2 is the biosorbed dye amount at equilibrium ($mg\,g^{-1}$) for the pseudo-second-order biosorption, q_t is the amount of dye biosorbed at time t ($mg\,g^{-1}$) and k_2 is the pseudo-second-order kinetic rate constant ($g\,mg^{-1}\,min^{-1}$). A plot of t/q_t vs. t should give a linear relationship for the applicability of the pseudo-second-order kinetic, as shown in Figs. 11 and 12. The rate constant (k_2) and adsorption at equilibrium (q_2) can be obtained from the intercept and slope, respectively.

The intraparticle diffusion equation [34] can be written as follows:

$$q_t = k_p t^{1/2} + C \tag{4}$$

where C is the intercept, and k_p is the intraparticle diffusion rate constant ($mg\,g^{-1}\,min^{-1/2}$) (Figs. 13 and 14). The results of the kinetic parameters for biosorption are given in Table 4. The correlation coefficients for the pseudo-second-order kinetic model for AB 225 and AB 062 were close to 1.0 for all cases. The correlation coefficients for the first-order kinetics and intraparticle diffusion equation models were lower than that the pseudo-second-order. These results indicate that the biosorption of AB 225 and AB 062 by *P. macerans* follows the pseudo-second-order kinetics model, which relies on the assumption that the rate-limiting step may be biosorption involving valence forces through the sharing or exchange of electrons between biosorbent and sorbate [35].

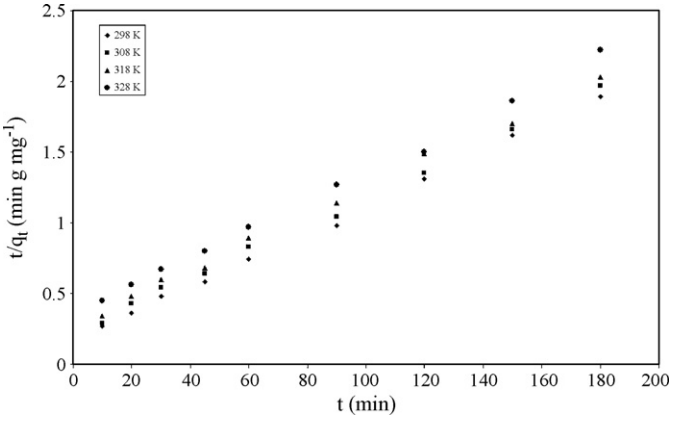

Fig. 12. Pseudo-second-order kinetic plots for the biosorption of AB 062 by *P. macerans* at various temperatures.

Table 4
Kinetic parameters for the adsorption of AB 225 and AB 062 onto *Paenibacillus macerans* at various temperatures.

Dyes	T (K)	q_{exp} (mg g^{-1})	k_1 (min^{-1})	q_1 (mg g^{-1})	r_1^2	k_2 ($\times 10^{-4}$ g mg^{-1} min^{-1})	q_2 (mg g^{-1})	r_2^2	k_p (mg g^{-1} min$^{-1/2}$)	C (mg g^{-1})	r_p^2
AB	298	89.13	22.62	108.70	0.997	4.66	105.26	0.999	5.60	28.15	0.869
225	308	84.11	23.84	101.01	0.991	4.26	101.01	0.997	5.53	22.99	0.879
	318	73.74	26.17	90.91	0.992	5.15	86.96	0.996	4.77	20.39	0.851
	328	69.23	26.13	86.21	0.995	4.97	84.03	0.998	4.64	18.55	0.881
AB	298	91.89	18.83	106.38	0.995	5.30	106.38	0.999	5.27	32.93	0.853
062	308	86.33	20.01	99.00	0.981	4.17	104.17	0.998	5.61	24.69	0.906
	318	79.01	23.97	97.08	0.990	3.41	103.09	0.997	5.71	19.05	0.931
	328	70.75	34.12	98.04	0.998	2.91	99.01	0.998	5.77	11.94	0.935

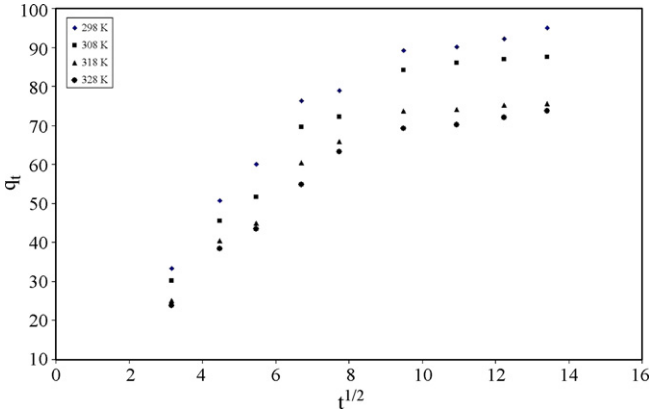

Fig. 13. Interparticle diffusion model plots for the biosorption of AB 225 by *P. macerans* at various temperatures.

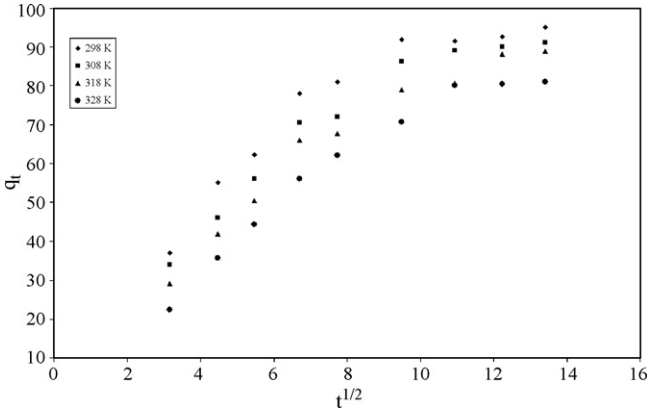

Fig. 14. Interparticle diffusion model plots for the biosorption of AB 062 by *P. macerans* at various temperatures.

3.7. Biosorption isotherms

Isotherms are the equilibrium relations between the concentration of the adsorbate on the solid phase and its concentration in the liquid phase. The equilibrium biosorption data have been analysed using Langmuir, Freundlich and Tempkin isotherms. Analysis of such isotherms is important in order to develop an equation that accurately represents the results and could be used for design purposes.

The Langmuir isotherm model assumes the uniform energies of adsorption onto the adsorbent surfaces. Furthermore, the Langmuir equation is based on the assumption of the existence of monolayer coverage of the adsorbate at the outer surface of the adsorbent where all sorption sites are identical. The Langmuir equation [36] is given as follows:

$$\frac{1}{q_e} = \frac{1}{q_{\max}} + \frac{1}{q_{\max} K_L} \frac{1}{C_e} \tag{5}$$

where q_e is the equilibrium dye concentration on the adsorbent (mg g^{-1}); C_e, the equilibrium dye concentration in solution (mg l^{-1}); $q_{\max}$, the monolayer capacity of the adsorbent (mg g^{-1}); K_L is the Langmuir constant. The plots of C_e/q_e vs. C_e for the biosorption of AB 225 and AB 062 onto *P. macerans* give a straight line of slope ($1/q_{\max}$) and intercept ($1/q_{\max}K_L$).

The essential features of Langmuir can be expressed in terms of dimensionless constant separation factor R_L which is calculated using the following equation [37]:

$$R_L = \frac{1}{1 + K_L C_0} \tag{6}$$

Values of R_L indicate the shapes of isotherms to be either unfavorable ($R_L > 1$), linear ($R_L = 1$), favorable ($0 < R_L < 1$).

The Freundlich isotherm model equation [38] is expressed as

$$\ln q_e = \ln K_F + \frac{1}{n} \ln C_e \tag{7}$$

Table 5
Adsorption isotherm constants for the adsorption of AB 225 and AB 062 onto *Paenibacillus macerans* at various temperatures.

Isotherm models	AB 225				AB 062			
	298 K	308 K	318 K	328 K	298 K	308 K	318 K	328 K
Langmuir								
K_L (l mg^{-1})	5.51×10^{-2}	2.87×10^{-2}	6.42×10^{-3}	1.93×10^{-4}	8.54×10^{-2}	5.14×10^{-2}	1.80×10^{-2}	7.57×10^{-3}
r_L^2	0.999	0.999	0.997	0.997	0.999	0.999	0.999	0.998
R_L	0.15	0.26	0.61	0.98	0.10	0.16	0.36	0.57
Freundluich								
$1/n$	0.50	0.60	0.99	1.01	0.44	0.49	0.65	0.80
K_F (l mg^{-1})	25.06	15.78	5.45	2.10	32.86	25.24	12.26	4.95
r_F^2	0.970	0.978	0.986	0.996	0.965	0.962	0.980	0.996
Tempkin								
B	55.53	64.33	84.18	93.78	48.64	54.45	68.29	75.55
A (l mg^{-1})	0.50	0.28	0.12	0.08	0.81	0.51	0.20	0.11
r_t^2	0.994	0.993	0.959	0.935	0.996	0.995	0.991	0.941

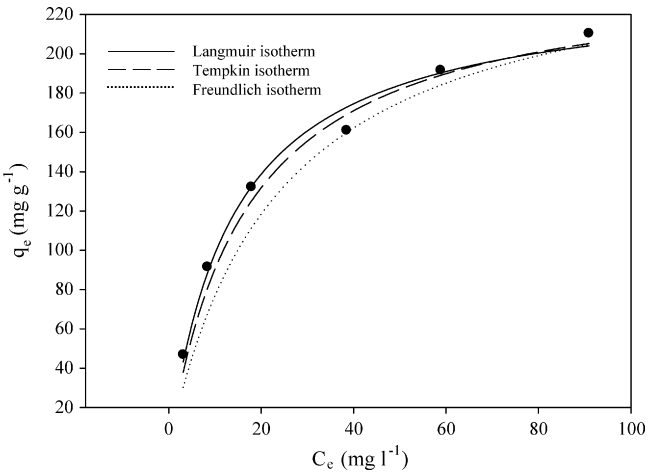

Fig. 15. Adsorption isotherms for AB 225 by *P. macerans* at 298 K.

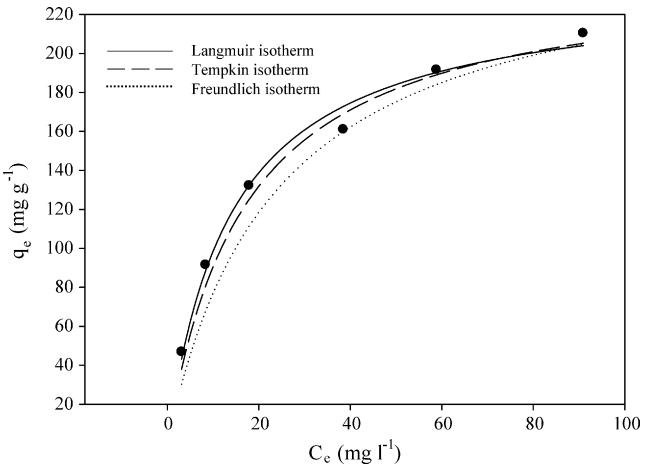

Fig. 16. Adsorption isotherms for AB 062 by *P. macerans* at 298 K.

where q_e is the equilibrium dye concentration on the adsorbent (mg g^{-1}); C_e, the equilibrium dye concentration in solution (mg l^{-1}); and K_F is the Freundlich constant. In this function, it is assumed that the sorbent has a surface with a non-uniform distribution of sorption heat. This equation was primarily proposed on a purely empirical basis for adsorption phenomena occurring on gas–solid interfaces, although it can be theoretically derived for an adsorption model in which the heat of adsorption varies exponentially with surface coverage. The slope of plot $1/n$ ranging 0 and 1, is a measure of adsorption intensity or surface heterogeneity, becoming more heterogeneous as its value gets closer to zero.

Tempkin and Pyzhev [39] considered the effect of some indirect sorbate/adsorbate interactions on the adsorption isotherm. This isotherm assumes that; the heat of adsorption of all the molecules in a layer decreases linearly with surface coverage of adsorbent due to sorbate–adsorbate interactions. This adsorption is characterized by a uniform distribution of binding energies. The linear form of the Tempkin isotherm equation [39] is represented by the following equation:

$$q_e = B \ln A + B \ln C_e \tag{8}$$

where $B = RT/b$, T is the absolute temperature in K, R the universal gas constant (8.314 J K^{-1} mol^{-1}), A the equilibrium binding constant and the constant B is related to the heat of adsorption. Values of B and A were calculated from the plot of q_e against $\ln C_e$.

The results of the isotherm parameters for the biosorption are given in Table 5 and Figs. 15 and 16. As shown in Table 5 that the correlation coefficients for the Langmuir isotherm model for AB 225 and AB 062 were close to 1.0 for all cases. The correlation coefficients for the Freundlich and Tempkin isotherm models were lower than that of the Langmuir isotherm model. Figs. 15 and 16 also confirm that the Langmuir isotherm has better fitting than the other isotherm models tested.

3.8. Thermodynamics parameters

In adsorption studies, both energy and entropy factors must be considered in order to determine which processes will occur spontaneously. The Gibbs free energy change, ΔG°, can be determined by the following equation:

$$\Delta G^\circ = -RT \ln K_L \tag{9}$$

where K_L is the Langmuir constant, R the universal gas constant (8.314 J K^{-1}mol^{-1}), and T is the absolute temperature (K). The relationship between Gibbs free energy change (ΔG°), entropy (ΔS°)

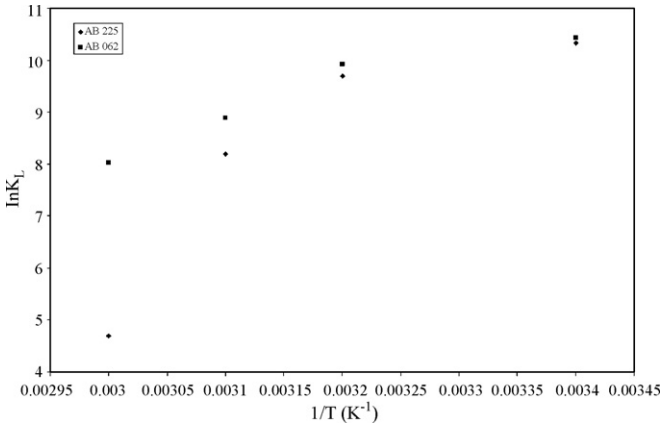

Fig. 17. Plots of $\ln K_L$ vs. $1/T$ for estimation of thermodynamic parameters.

and enthalpy change (ΔH°) is expressed as

$$\Delta G^\circ = \Delta H^\circ - T\,\Delta S^\circ \tag{10}$$

Eq. (10) can be expressed in its linear form as

$$\ln K_L = -\frac{\Delta H^\circ}{RT} + \frac{\Delta S^\circ}{R} \tag{11}$$

Thermodynamics parameters were calculated from the plot of $\ln K_L$ against $1/T$. The plots give a straight line of slope ($1/q_{max}$) and intercept ($1/q_{max}K_L$) as shown in Fig. 17. The results of thermodynamics parameters are shown in Table 6. The negative values of Gibbs free energy indicate that the adsorption of both dyes by *P. macerans* is spontaneous in nature.

Table 6
Thermodynamic parameters.

Dyes	T (K)	ΔG° (kJ mol^{-1})	ΔH° (kJ mol^{-1})	ΔS° (J mol^{-1} K^{-1})
AB 225	298	−25.62	−107.72	−273.62
	308	−24.81		
	318	−21.65		
	328	−12.79		
AB 062	298	−25.87	−50.07	−81.50
	308	−25.43		
	318	−23.50		
	328	−21.87		

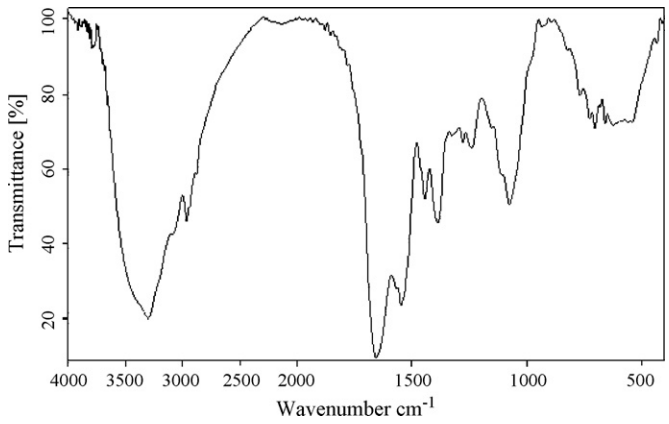

Fig. 18. FT-IR spectra of *P. macerans*.

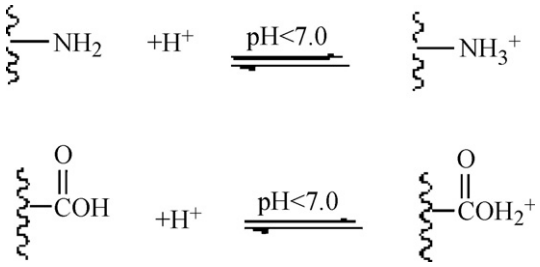

Fig. 19. Mechanism for removal acidic dyes on *P. macerans*.

3.9. FT-IR characterization of the biomass

In order to explain biosorption mechanism of the biomass, a FT-IR study was carried out. The FT-IR spectra of *P. macerans* are shown in Fig. 18. The FT-IR spectrum of the biomass displays the presence of functional groups at around 3200–3500 cm^{-1}, 2964 cm^{-1}, 1658 cm^{-1}, 1548 cm^{-1} and 1075 cm^{-1} absorption peaks. The broad absorption peaks at around 3200–3500 cm^{-1} indicates the presence of carboxylic acid and amino groups. The absorption peak at 2964 cm^{-1} confirmed existence C–H stretching vibration. The stretching vibration band 1658 cm^{-1} is due to carbonyl group (C=O). The absorption peak at 1548 cm^{-1} also supported presence of amino group. The band at 1075 cm^{-1} shows C–O stretching vibration.

The mechanism for removal acidic dyes from aqueous solution is shown in Fig. 19. According to the estimated mechanism, carboxylic acid, carbonyl and amino groups are protonated at pH less than 7, therefore, the number of positively charged sites increases. Thereby the biosorption of acidic dyes increase. This can be explained by the electrostatic attraction between the positively charged surface ($-COOH_2^+$, NH_3^+) and the negative sulfonate ($-SO_3^-$) groups of dye molecule in acidic medium.

4. Conclusion

This paper reports kinetic, equilibrium and thermodynamic studies on biosorption of AB 225 and AB 062 by *P. macerans*. The maximum biosorption capacities of AB 225 and AB 062 onto *P. macerans* biomass were 94.98 mg g^{-1} and 95.08 mg g^{-1}, respectively, at optimum conditions of pH (1.0) and temperature (25 °C) according to Langmuir isotherm model and pseudo-second-order kinetic model. The biosorption equilibrium was reached in 90 min.

Thermodynamic parameters showed that the biosorption process is exothermic and spontaneous. The negative value of entropy ΔS° indicates the decreased randomness at the solid–liquid interface during the sorption of dyes onto *P. macerans*.

The presence of carboxylic groups and other groups were identified as components of *P. macerans* structure by FT-IR analysis. The results indicated that the biosorption system could be explained by the electrostatic attraction between the positively charged surface and the negatively dye molecule in acidic medium *P. macerans* can become a suitable alternative sorbent for removing acid dyes from wastewaters.

Acknowledgement

The authors gratefully acknowledge the help received from Dr. Semra İlhan, University of Osmangazi, Eskişehir, Turkey.

References

[1] M. Šafaříková, L. Ptáčková, I. Kibriková, I. Šafařík, Biosorption of water-soluble dyes on magnetically modified Saccharomyces cerevisiae subsp. uvarum cells, Chemosphere 59 (6) (2005) 831–835.
[2] S.V. Mohan, N.C. Rao, K.K. Prasad, J. Karthikeyan, Treatment of simulated Reactive Yellow 22 (azo) dye effluents using *spyrogyra* species, Waste Manage. 22 (2002) 575–582.
[3] A. Ozer, G. Akkaya, M. Turabik, The biosorption of Acid Red 337 and Acid Blue 324 on *Enteromorpha prolifera*: the application of nonlinear regression analysis to dye biosorption, Chem. Eng. J. 112 (2005) 181–190.
[4] Y.C. Wong, Y.S. Szeto, W.H. Cheung, G. McKay, Adsorption of acid dyes on chitosan equilibrium isotherm analyses, Process Biochem. 39 (2004) 695–704.
[5] P.K. Malik, Use of activated carbons prepared from sawdust and rice-husk for adsorption of acid dyes: a case study of Acid Yellow 36, Dyes Pigments 56 (2003) 239–249.
[6] K. Vasanth Kumar, K. Porkodi, Mass transfer, kinetics and equilibrium studies for the biosorption of methylene blue using *Paspalum notatum*, J. Hazard. Mater. 46 (2007) 214–226.
[7] E. Weber, N.L. Wolfe, Kinetics studies of reduction of aromatic azo compounds in anaerobic sediment/water systems, Environ. Toxicol. Chem. 6 (1987) 911–920.
[8] I. Kiran, T. Akar, A. Safa Ozcan, A. Ozcan, S. Tunali, Biosorption kinetics and isotherm studies of Acid Red 57 by dried *Cephalosporium aphidicola* cells from aqueous solutions, Biochem. Eng. J. 31 (2006) 197–203.
[9] R. Gong, Y. Ding, M. Li, C. Yang, H. Liu, Y. Sun, Utilization of powdered peanut hull as biosorbent for removal of anionic dyes from aqueous solution, Dyes Pigments 64 (2005) 187–192.
[10] T. Robinson, B. Chandran, P. Nigam, Removal of dyes from a synthetic textile dye effluent by biosorption on apple pomace and wheat straw, Water Res. 36 (2002) 2824–2830.
[11] T. Robinson, G. Mcmullan, R. Marchant, P. Nigam, Remediation of dyes in textile effluent: a critical review on current treatment technologies with a proposed alternative, Bioresour. Technol. 77 (2001) 247–255.
[12] R.-S. Juang, R.-L. Tseng, F.-C. Wu, S.-H. Lee, Adsorption behaviour of reactive dyes from aqueous solutions on chitosan, J. Chem. Technol. Biotechnol. 70 (1997) 391–399.
[13] S. Karcher, A. Kornmuller, M. Jekel, Removal of reactive dyes by sorption/complexation with cucurbituril, Water Sci. Technol. 40 (1999) 425–433.
[14] Z. Aksu, S. Tezer, Equilibrium and kinetic modelling of biosorption of Remazol Black B by *R. arrhizus* in a batch system: effect of temperature, Process Biochem. 36 (2000) 431–439.
[15] T. O'Mahony, E. Guibal, J.M. Tobin, Reactive dye biosorption by *Rhizopusarrhizus* biomass, Enzyme Microbial Technol. 31 (2002) 456–463.
[16] Z. Aksu, Application of biosorption for the removal of organic pollutants: a review, Process Biochem. 4 (2005) 997–1026.
[17] M.M. Figueria, B. Volesky, K. Azarian, V.S.T. Ciminelli, Biosorption column performance with a metal mixture, Environ. Sci. Technol. 34 (2000) 4320–4326.
[18] Y. Fu, T. Viraraghavan, Fungal decolourization of wastewaters: a review, Bioresour. Technol. 79 (2001) 251–262.
[19] Y. Fu, T. Viraraghavan, Removal of Congo Red from an aqueous solution by fungus *Aspergillus niger*, Adv. Environ. Res. 7 (2002) 239–247.
[20] Y. Fu, T. Virarahavan, Removal of a dye from an aqueous solution by the fungus *Aspergillus niger*, Water Qual. Res. J. Can. 35 (2000) 95–111.
[21] Y. Fu, T. Virarahavan, Removal of C.I. Acid Blue 29 from an aqueous solution by *Aspergillus niger*, AATCC Mag. 1 (2001) 36–40.
[22] Y. Fu, T. Viraraghavan, Dye biosorption sites in *Aspergillus niger*, Bioresour. Technol. 82 (2002) 139–145.
[23] Z. Aksu, Sevilay Tezer Biosorption of reactive dyes on the green alga Chlorella vulgaris, Process Biochem. 40 (2005) 1347–1361.
[24] P.H.A. Sneath, Endospore forming gram positive rods and cocci, Bergeys Manuel Syst. Bacteriol. 2 (1986) 1104–1207.
[25] M. Sasser, Identification of bacteria by gas chromatography of cellular fatty acids, MIDI Technical Note 101 (1990) 199–204.
[26] M.S. Chiou, G.S. Chuang, Competitive adsorption of dye metanil yellow and RB15 in acidic solutions on chemically cross-linked chitosan beads, Chemosphere 62 (2006) 731–740.
[27] K.A. Gallagher, M.G. Healy, S.J. Allen, Biosorption of synthetic dye and metal ions from aqueous effluents using fungal biomass, in: D.L. Wise (Ed.), Global Environmental Biotechnology, Elsevier, UK, 1997, pp. 27–50.

[28] F. Banat, S. Al-Asheh, L. Al-Makhedmeh, Evaluation of the use of raw and activated date pits as potential adsorbents for dye containing waters, Process Biochem. 39 (2003) 193–202.
[29] A. Ozer, D. Ozer, H.I. Ekiz, Application of Freundlich and Langmuir models to multistage purification process to remove heavy metal ions by using *Schizomeris leibleinii*, Process Biochem. 34 (1999) 919–927.
[30] A. Shukla, Y. Zhang, P. Dubey, J.L. Margrave, S.S. Shukla, The role of sawdust in the removal of unwanted materials from water, J. Hazard. Mater. B 95 (2002) 137–152.
[31] G. Donmez, Z. Aksu, Removal of chromium (VI) from saline wastewaters by Dunaliella species, Process Biochem. 38 (2002) 751–762.
[32] N. Kannan, M.M. Susndaram, Kinetics and mechanism of removal of methylene blue by adsorption on various carbons—a comparative study, Dyes Pigments 51 (2001) 25–40.
[33] Y.S. Ho, G. McKay, Kinetic models for the sorption of dye from aqueous solution by wood, Process Saf. Environ. Protect. 76 (1998) 183–191.
[34] W.J. Weber Jr., J.C. Morriss, Kinetics of adsorption on carbon from solution, J. Sanitary Eng. Div. Am. Soc. Civil Eng. 89 (1963) 31–60.
[35] Y.S. Ho, G. McKay, Sorption of dye from aqueous solution by peat, Chem. Eng. J. 70 (1998) 115–124.
[36] I. Langmuir, The adsorption of gases on plane surfaces of glass, mica and platinum, J. Am. Chem. Soc. 40 (1918) 1361–1403.
[37] T.W. Webi, R.K. Chakravort, J. Am. Inst. Chem. Eng. 20 (2) (1974) 228.
[38] H.M.F. Freundlich, Über die adsorption in LÖsungen, C. Phys. Chem. 57 (1906) 385–470.
[39] M.J. Tempkin, V. Pyzhev, Kinetics of ammonia synthesis on promoted iron catalysis, Acta Physiochim. URSS 12 (1940) 327–356.